Carbohydrate Research 346 (2011) 949–955

Contents lists available at ScienceDirect

Carbohydrate Research

journal homepage: www.elsevier.com/locate/carres

An improved synthetic approach to 7-[3-amino-4-*O*-(α-L-mycarosyl)-2,3,6-trideoxy-α-L-*lyxo*-hexopyranosyl]daunorubicinone and its interaction with human serum albumin

Xiaoyun Dang [a], Qingfeng Liu [b,c], Fengling Cui [b,*], Lixia Qin [b], Guisheng Zhang [b,c,*], Xiaojun Yao [d], Juan Du [d]

[a] College of Physical Education, Henan Normal University, 46 East Construction Road, Xinxiang, Henan 453007, PR China
[b] College of Chemistry and Environmental Sciences, Henan Normal University, 46 East Construction Road, Xinxiang, Henan 453007, PR China
[c] Key Laboratory of Green Chemical Media and Reactions of Ministry of Education, Henan Normal University, 46 East Construction Road, Xinxiang, Henan 453007, PR China
[d] Department of Chemistry, Lanzhou University, Lanzhou 730000, PR China

ARTICLE INFO

Article history:
Received 25 November 2010
Received in revised form 30 January 2011
Accepted 2 February 2011

Keywords:
7-[3-Amino-4-*O*-(α-L-mycarosyl)-2,3,6-trideoxy-α-L-*lyxo*-hexopyranosyl]-daunorubicinone
Human serum albumin
Fluorescence quenching
Molecular modeling
Synchronous fluorescence

ABSTRACT

An improved synthetic approach to 7-[3-amino-4-*O*-(α-L-mycarosyl)-2,3,6-trideoxy-α-L-*lyxo*-hexopyranosyl]daunorubicinone (α**1**) with high stereoselectivity and good yield was developed. The feature of its binding to human serum albumin (HSA) was also investigated under simulative physiological conditions via fluorescence and UV–vis absorption spectroscopy and molecular modeling methods. The results revealed that α**1** caused the fluorescence quenching of HSA by the formation of α**1**–HSA complexes. Hydrophobic interactions played a major role in stabilizing the complex, which was in good agreement with the results of the molecular modeling study. In addition, the effect of common ions on the binding constants of α**1**–HSA complexes at room temperature was also discussed. All the experimental results and theoretical data indicated that α**1** bound to HSA and was effectively transported and eliminated in the body. Such findings may provide useful guidelines for further drug design.

1. Introduction

The anthracycline quinone antibiotics daunorubicin (DNR) and doxorubicin are potent antitumor agents that show activity against a variety of solid tumors.[1] The major problems associated with anthracycline drugs are cardiotoxicity and drug resistance mediated by a multidrug resistance gene. Many researchers have modified the structure of anthracyclines to generate analogs with the aim of reducing the side effects and reverse multidrug resistance; however, these efforts have shown only limited success. Recently, Zhang and co-workers have reported a novel class of disaccharide analogs of DNR that are effective against leukemia cells.[2,3] In these disaccharide analogs the first (inner) sugar in the carbohydrate chain is a daunosamine, and the second group of sugars that are linked to the first sugar is a series of uncommon sugars. Of all these disaccharide anthracyclines, the compounds with an α-configuration at the terminal 2,6-dideoxy sugar, including α**1** (Scheme 1), show potent anticancer activities and higher topoisomerase II targetability than the parent compound DNR. They are worthy of further evaluation as new drug candidates. Very interestingly, α**1** with an α-configuration at the terminal 2,6-dideoxy sugar moiety shows 35-fold higher cytotoxicity than β**1** (Scheme 1) with the β-configuration. In the previous work,[2] α**1** and β**1** were obtained in a ratio of 2:1. In the key synthetic process, the glycosylation of **2** with glycosyl donor **5** produced the precursor α-**6** and β-**6** in yields of 40% and 20%, respectively. It is necessary to improve the method to enhance the stereroselectivity and yield.

Drug–protein interactions in the blood stream may strongly affect the distribution, free concentration, and the metabolism of various drugs. This type of interaction can also influence drug stability and toxicity during the chemotherapeutic process. Serum albumins are the most abundant proteins in plasma. As the major soluble protein constituents of the circulatory system, serum albumins have many physiological functions and play a dominant role in drug disposition and efficacy.[4,5] They often increase the apparent solubility of hydrophobic drugs in plasma and modulate their delivery to cells in vivo and in vitro. Consequently, it is important to know the affinity of a drug to serum albumin, even if it is not the only factor to predict serum concentrations of the free drug.

Human serum albumin (HSA), the main protein component in the blood serum, is a globular protein composed of a single polypeptide chain of 585 amino acid residues with a large α-helix. HSA binds strongly to many kinds of endogenous and exogenous

* Corresponding author. Tel./fax: +86 373 3326336.

0008-6215/$ - see front matter © 2011 Published by Elsevier Ltd.
doi:10.1016/j.carres.2011.02.005

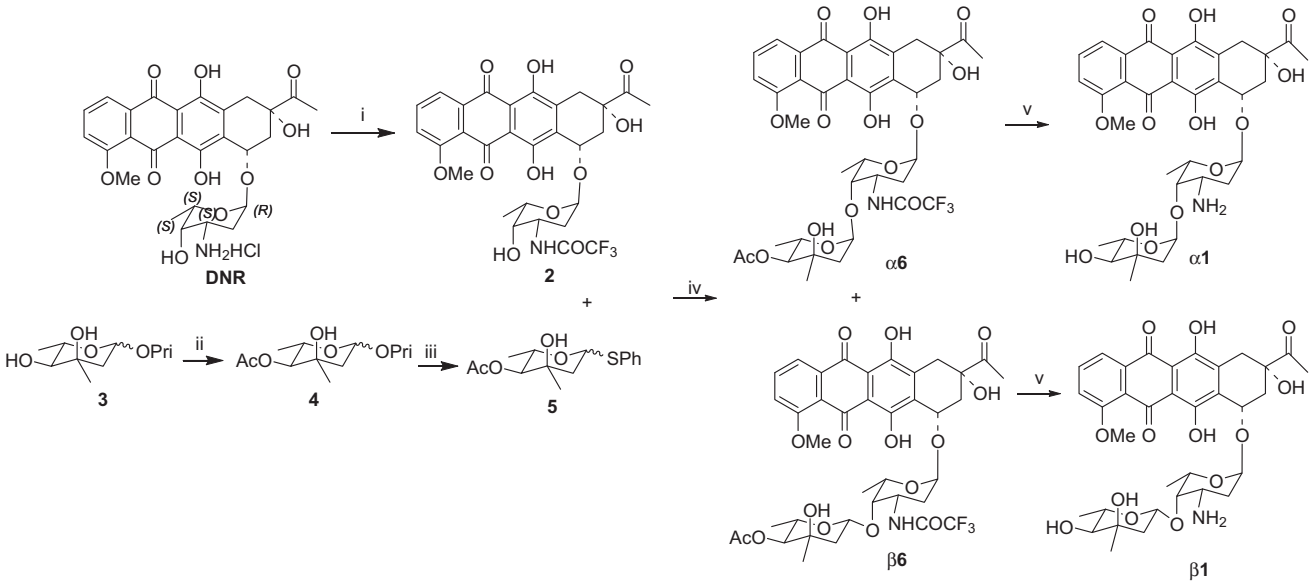

Scheme 1. Reagents and conditions: (i) $(CF_3CO)_2O$/pyridine, −20 °C, 15 min, 95% yield; (ii) Ac_2O/pyridine, rt, 24 h, 90% yield; (iii) PhSH, $BF_3{\cdot}Et_2O/CH_2Cl_2$, 0 °C, 2 h, 97% yield; (iv) NIS, TfOH, 4 Å MS, 2–8 h (65% yield, α**6**/β**6** = 12:1); (v) 0.1 M NaOH/THF, 0 °C, 6 h, 75% yield.

substances and is thus the most important carrier for drugs and endogenous substances in the blood.[6] Binding of drugs to plasma proteins is an important pharmacological parameter since very strong albumin binding diminishes the active concentration of a drug in plasma and leads to a competitive release of other drugs bound to albumin that are administered in the same time frame.[7] The subsequent increase of the concentration of the released drug may lead to serious drug–drug interactions; therefore, a very high affinity to HSA is usually undesirable in potential drugs.[8] The studies on HSA–drug interactions may provide some important information of the structural features that determine the therapeutic effectiveness of drugs.

Fluorescence quenching is an important method to study the interaction of substances with protein because it is sensitive and relatively easy to use. Fluorescence spectroscopy is essentially a probe technique that senses changes in the local environment of the fluorophore, which distinguishes it from other techniques, such as calorimetry, far-UV circular dichroism (CD), and infrared (IR) spectroscopy. Also, various possibilities of structural rearrangements in the environment of the fluorophore may lead to a similar fluorescence signal, which can complicate interpretation of the experimental result and be exploited to obtain unique structural and dynamic information.[9–11] In the present work, we demonstrate the binding of α**1** to HSA by using fluorescence quenching, UV–vis absorption spectroscopy, and molecular modeling. The nature of the binding of α**1** to HSA is described. The effect of the energy transfer was studied according to the Förster theory of non-radiation energy transfer.

2. Materials and methods

2.1. Materials

Appropriate amounts of human serum albumin (Hualan Biological Engineering Ltd) was directly dissolved in water to prepare a stock solution at a final concentration of 2.0×10^{-5} M and stored in the dark at 0–4 °C. A 2.89×10^{-4} M solution of α**1**, a 0.5 M NaCl working solution, a 0.1 M Tris–HCl buffer solution of pH 7.4 and other ionic solutions were prepared. All chemicals were of analytical reagent grade and were used without further purification. Double-distilled water was used throughout the experiments.

2.2. Apparatus

All fluorescence spectra were recorded on an FP-6200 spectrofluorimeter (JASCO, Japan) and a RF-540 spectrofluorimeter (Shimadzu, Japan) equipped with a thermostated bath, using 5 nm/5 nm slit widths. The UV absorption spectra were performed on a Tu-1810 UV–vis spectrophotometer. The pH values were measured on a pH-3 digital pH meter with a glass combination electrode. All calculations for molecular modeling were performed on an SGI workstation.

2.3. Preparation of α1

The synthetic pathway of α**1** is outlined in Scheme 1. Intermediates **2** and **5** were synthesized according to the known procdures.[2] The precursor α**6** was prepared via an improved procedure using TfOH/*N*-iodosuccinimide (NIS) instead of $AgPF_6$–2,4,6-*tert*-butylpyrimidine (TTBP) as an activating system: a mixture of 2,6-dideoxythioglycoside **5** (0.48 mmol), compound **2** (0.4 mmol), NIS (0.48 mmol), and 4 Å molecular sieves in dry CH_2Cl_2 (10 mL) was stirred for 1 h at rt. Then a satd solution of TfOH in CH_2Cl_2 (0.31 mL, 0.047 mmol) was added dropwise at 0 °C. When the reaction was completed (monitored by TLC), the reaction mixture was diluted with CH_2Cl_2 (10 mL), and washed with satd aq $Na_2S_2O_3$ and brine, then concentrated on a rotary evaporator. The resulting residue was purified by column chromatography on silica gel (1:75 MeOH–CH_2Cl_2) to give α**6** as a red solid in 60% yield: ^{1}H NMR (400 MHz, $CDCl_3$): δ 13.90 (1H, s, HO-6), 13.81 (1H, s, HO-11), 7.99 (1H, d, J = 8.8 Hz, $NHCOCF_3$), 7.87 (1H, d, J = 7.6 Hz, H-1), 7.66 (1H, t, J = 8.0 Hz, H-2), 7.30 (1H, d, J = 7.6 Hz, H-3), 5.44 (1H, d, J = 3.3 Hz, H-1′), 5.14 (1H, s, H-7), 4.97 (1H, br, J = 3.5 Hz, H-1″), 4.65 (1H, d, J = 9.9 Hz, H-4″), 4.20–4.18 (4H, m, H-3′, H-5′, H-5″, H-4′), 3.99 (3H, s, OMe-4), 3.61(1H, s, OH-9), 3.09 (1H, d, J = 18.9 Hz, Ha-10), 2.80 (1H, d, J = 18.9 Hz, Hb-10), 2.35 (3H, s, H-14), 2.10, 1.91, (9H, m, H-8, H-2′, H-2″, OAc), 1.27 (3H, d, J = 6.2 Hz, H-6′), 1.45 (6H, m, CH_3-3″, H-6″). HR-ESIMS (positive-ion mode): calcd for $C_{38}H_{42}F_3NO_{15}Na^+$, m/z 832.2398, found, m/z 832.2468. The final product α**1** was obtained by mild deprotection of α**6** with 0.1 M NaOH in THF following the known procedure.[2] Purification of the crude product on a column of silica gel (1:25–1:10 MeOH–CH_2Cl_2) gave α**1** as a deep-red solid

(75%): ^{1}H NMR (400 MHz, $CDCl_3$): δ 7.86 (1H, d, J = 7.6 Hz, H-1), 7.69 (1H, t, J = 8.0 Hz, H-2), 7.27 (1H, d, J = 8.4 Hz, H-3), 5.40 (1H, d, J = 3.0 Hz, H-1′), 5.10 (1H, br, H-7), 4.92 (1H, J = 2.6 Hz, H-1″), 4.07 (1H, m, H-5′), 3.97 (3H, s, OMe-4), 3.86 (1H, m, H-5″), 3.50 (1H, br, H-4′), 3.07–3.05 (2H, m, Ha-10, H-3′), 2.94 (1H, d, J = 79.6 Hz, H-4″), 2.79 (1H, d, J = 18.7 Hz, Hb-10), 2.34 (3H, s, H-14), 2.16–2.14 (2H, m, Ha-2″, Ha-8), 2.01–1.99 (1H, m, Hb-8), 1.82–1.78 (1H, m, Hb-2″), 1.68–1.66 (2H, m, H-2′), 1.25–1.21 (9H, m, H-6′, H-6″, CH_3-3″). HRESIMS (positive-ion mode): calcd for $C_{34}H_{41}NO_{13}Na^+$, m/z 694.2470, found, m/z 694.2463.

2.4. Measurements of the fluorescence spectrum

Under the optimum physiological conditions described above, 2.0 mL Tris–HCl buffer solution, 2.0 mL NaCl solution, appropriate amounts of HSA, and α1 were added into a standard flask and diluted to 10.0 mL with double-distilled water. Fluorescence quenching spectra of HSA were obtained at an excitation wavelength of 280 nm and an emission wavelength of 300–450 nm. Fluorescence spectra in the presence of other ions were also measured under the same conditions. In addition, the UV absorption and synchronous fluorescence spectra of system were recorded.

2.5. Principles of fluorescence quenching

The fluorescence intensity of a compound can be decreased by a variety of molecular interactions that include the following: excited-state reactions, molecular rearrangement, energy transfer, ground-state complex formation, and collisional quenching.[12] Fluorescence quenching is described by the Stern–Volmer equation (Eq. 1):

$$F_0/F = 1 + K_q\tau_0[Q] = 1 + K_{sv}[Q], \quad (1)$$

where F_0 and F are the fluorescence intensities before and after the addition of the quencher, respectively. K_q, K_{SV}, τ_0, and [Q] are the quenching rate constant of the biomolecule, the Stern–Volmer dynamic quenching constant, the average lifetime of the biomolecule without quencher ($\tau_0 = 10^{-8}$ s), and the concentration of the quencher, respectively. The concentration of the quencher should be the free ligand concentration, but it is not known in the experiment. So, in our analysis it was approximated by the total concentration of the quencher. For higher ligand concentrations, in excess of available specific protein binding sites, this approximation is valid. Obviously,

$$K_q = K_{sv}/\tau_0. \quad (2)$$

Hence, Eq. 1 is applied to determine K_{SV} by linear regression of a plot of F_0/F against [Q]. In many instances, the fluorophore can be quenched both by collision and by complex formation with the same quencher. In these cases, the Stern–Volmer plot exhibits an upward curvature, concave toward the y-axis at high [Q], and F_0/F is related to [Q] by the following form of the Stern–Volmer equation:[13]

$$F_0/F = (1 + K_D[Q])(1 + K_S[Q]), \quad (3)$$

where K_D and K_S are the dynamic and static quenching constants, respectively. The first factor on the right-hand side in Eq. 3 describes the 'dynamic' quenching, resulting from encounters of quencher and fluorophore during the excited state, and the second factor describes the 'static' quenching, that is the quenching caused by the formation of a complex between the quencher and the fluorophore predating the excitation. This modified form of the Stern–Volmer equation is second order with respect to [Q], which accounts for the upward curvature observed at high [Q] when both static and dynamic quenching occur for the same fluorophore.

2.6. Calculation of binding parameters

The binding constants can be found from the static quenching equation:

$$(F_0 - F)^{-1} = F_0^{-1} + K^{-1}F_0^{-1}[Q]^{-1}, \quad (4)$$

where K (intercept/slope) denotes the binding constant of **α1** and the biomolecule, which can be calculated from the slope and intercept of Lineweaver–Burk curves, F_0 and F are the fluorescence intensities without and with quencher, and [Q] is the quenching rate constant of the biomolecule.

If the enthalpy change (ΔH) does not vary significantly over the temperature range studied, then its value and that of ΔS can be determined from the Van't Hoff equation:[14]

$$\ln K = -\Delta H/RT + \Delta S/R. \quad (5)$$

In Eq. 5, K is the binding constant at corresponding temperature and R is the gas constant. The enthalpy change (ΔH) and the entropy change (ΔS) are calculated from the slope and ordinate of the Van't Hoff relationship. The free-energy change (ΔG) is estimated from the following relationship:

$$\Delta G = \Delta H - T\Delta S = -RT\ln K. \quad (6)$$

2.7. Characteristics of synchronous fluorescence method

The synchronous fluorescence spectra were obtained by simultaneously scanning the excitation and emission monochromators. Thus, the synchronous fluorescence applied to the equation of synchronous luminescence:[15]

$$F = kcdE_{ex}(\lambda_{em} - \Delta\lambda)E_{em}(\lambda_{em}), \quad (7)$$

where F is the relative intensity of synchronous fluorescence, $\Delta\lambda = \Delta\lambda_{em} - \lambda_{ex}$ is a constant, E_{ex} is the excitation function at the given excitation wavelength, E_{em} is the normal emission function at the corresponding emission wavelength, c is the analytical concentration, d is the thickness of the sample cell, and k is the characteristic constant comprising the 'instrumental geometry factor' and related parameters. Since the relationship of the synchronous fluorescence intensity (F) and the concentration of **α1** should follow the F equation, F should be in direct proportion to the concentration of **α1**.

The optimal values of the wavelength intervals ($\Delta\lambda$) are important for the correct analysis and interpretation of the binding mechanism. When the wavelength interval ($\Delta\lambda$) is fixed at 60 nm of protein, the synchronous fluorescence has the same intensity as the emission fluorescence following excitation at 280 nm; only the emission maximum wavelength and shape of the peaks were changed.[16–18] Thus, these synchronous fluorescence measurements can be applied to calculate association constants similar to the emission fluorescence measurements. Therefore, the synchronous fluorescence measurements can deduce the binding mechanism as the emission fluorescence measurements did. In this study, the synchronous fluorescence spectra of tyrosine residues and tryptophan residues were measured at λ_{em} = 280 nm ($\Delta\lambda$ = 15 and 60 nm) in the absence and in the presence of various amounts of **α1**.

2.8. HSA–α1 docking study

The crystal structure of HSA in complex with R-warfarin was taken from the Brookhaven Protein Data Bank (entry codes 1h9z). The potential of the 3D structure of HSA was assigned according to the Amber 4.0 force field with Kollman all-atom charges. The initial structures of all the molecules were generated by the

molecular modeling software, SYBYL 6.9.1.[19] The geometry of the molecule was subsequently optimized using the Tripos force field with Gasteiger–Marsili charges. The FLEXX program was applied to calculate the possible conformation of the drug that binds to the protein. The PDB file contains a co-crystal with a small ligand (R-warfarin) in the active site. This ligand was extracted and used as a reference structure (a fixed conformation docked into the active site of the HSA). FLEXX program also did an RMS (root-mean-square) comparison between the reference structure and final docked structure of α1 as an indication of accuracy. The receptor descriptor file (rdf) lies at the heart of FLEXX. It contains the information about the protein, its amino acids, the active site, non-amino acid residues, and specific torsion angles. The SYBYL interface to FLEXX created a default rdf file. As the last step, the FLEXX program was used to build the interaction modes between the α**1** and HSA. Compound α**1** was docked to HSA by FLEXX, and then it revealed hydrogen bonds between α**1** and some residues of HSA. The calculation was performed through SGI FUEL workstations.

3. Results and discussion

3.1. Chemistry

In the previous work,[2] the glycosylation of intermediate **2** was performed using $AgPF_6$–TTBP as the promoter, which afforded the key intermediate α-**6** and the isomer β-**6** in yields of 40% and 20%, respectively. The selectivity for the preparation of α**1** was still unsatisfactory. It is necessary to improve the method to enhance the stereroselectivity and yield of α-**6**. Thioglycoside donors are believed to be the best choice for the α-glycosylation of 2,6-dideoxy sugars as they are stable to normal protecting-group manipulation, and various activating systems can be applied. On scrutinizing various activating systems, finally, we were satisfied with the results obtained by NIS–TfOH. The mixture of intermediate **2** and glycosyl donor **5**, in the presence of NIS and molecular sieves (4 Å, <5 μm, freshly activated), was treated with TfOH at 0 °C to give the glycosylated products in 65% yield and high selectivity (α**6**/β**6** = 12:1, Scheme 1).

3.2. Biology

3.2.1. Fluorescence quenching and binding constants

HSA is a single, 66 kDa monomeric polypeptide of 585 amino acidic residues, stabilized by 17 disulfide bridges. HSA contains three homologous α-helix domains (I–III). Each domain contains 10 helices and is divided into antiparallel six-helix and four subdomains (A and B).[20,21] A valuable feature of the intrinsic fluorescence of proteins is the high sensitivity of tryptophan to its local environment.[13] Changes in the emission spectra of tryptophan are common in response to protein conformational transitions, subunit association, substrate binding, or denaturation.[10] So, the intrinsic fluorescence of proteins can provide considerable information about their structure and dynamics, and it is often considered in the studies of protein folding and association reactions. There is only one tryptophan located at position 214 along the chain, in subdomain IIA of HSA. HSA solutions excited at 290 nm emit fluorescence attributable mainly to tryptophan residues.

The effect of α**1** on tryptophan residue fluorescence intensity is shown in Figure 1. As the data show, the fluorescence intensity of HSA decreases regularly with the increasing concentration of α**1**, which indicates that α**1** can bind to the HSA, and the binding site of α**1** on HSA is adjacent to the sole tryptophan residue of HSA. In order to discuss the results within the linear concentration range, we have carried out selectively the experiment within the linear part of the Stern–Volmer dependence (F_0/F vs [Q]). Figure 2

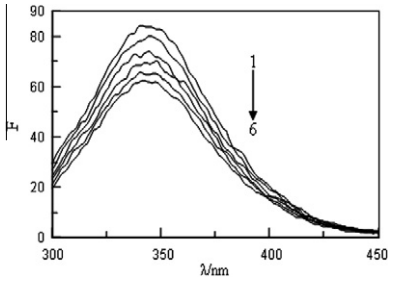

Figure 1. The fluorescence spectra of α**1**–HSA system (from **1** to **6**: $C_{HSA} = 1.2 \times 10^{-6}$ M; $C_{\alpha 1} = 0, 5.78, 11.56, 17.34, 23.12, 28.90 \times 10^{-6}$ M).

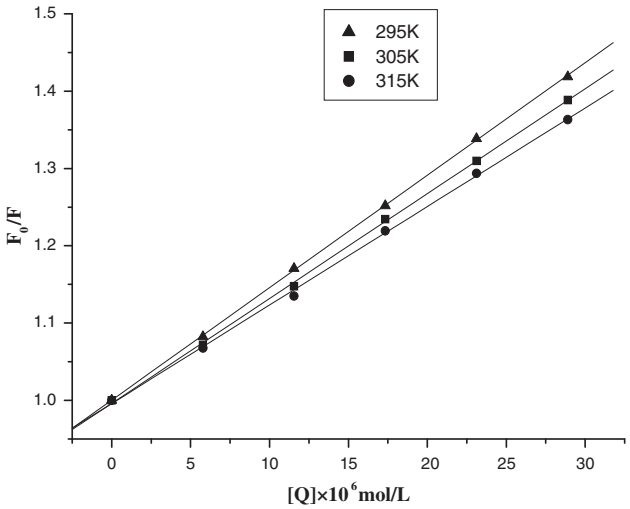

Figure 2. The Stern–Volmer curves for quenching of α**1** with HSA.

Table 1
The dynamic quenching constants (L/mol/s) between α**1** and HSA

T (K)	Stern–Volmer equation	K_q (L mol^{-1} S^{-1})	R
294	$Y = 1.02998 + 1.455 \times 10^4$ [Q]	1.455×10^{12}	0.9993
304	$Y = 1.00792 + 1.357 \times 10^4$ [Q]	1.357×10^{12}	0.9997
314	$Y = 0.99961 + 1.274 \times 10^4$ [Q]	1.274×10^{12}	0.9995

displays the Stern–Volmer plots of the quenching of HSA tryptophan residue fluorescence by α**1** at different temperatures. The plot shows that the results agree with the Stern–Volmer Eq. 1 within the investigated concentrations. The Stern–Volmer relationship does not show deviation toward the *y*-axis obviously at the experimental concentration range, which is an indication that either dynamic quenching or static quenching is predominant. The binding constants obtained from the Stern–Volmer method are listed in Table 1. The results show that the Stern–Volmer dynamic quenching constant K_{SV} is inversely correlated with temperature, which indicates that the probable quenching mechanism of fluorescence of HSA by α**1** is not initiated by dynamic collision but by complex formation.[13] In other words, the fluorescence quenching of HSA that results from complex formation is predominant, while that from dynamic collision could be negligible. The binding constants calculated by Eq. 4 and the slope and intercept of the Lineweaver–Burk curves are shown in Table 2 and Figure 3. They show a reasonably strong binding constant between α**1** and HSA, and the association constant decreases with increasing temperature, but the effect of temperature on the association constants is small. Thus, the quenching efficiency of α**1** to HSA is not obviously reduced when the experimental temperature is increased.

Table 2
The binding constants (L mol^{-1}) between **α1** and HSA at different temperatures

T (K)	Lineweaver–Burk equation	K (L mol^{-1})	R
294	$Y = 0.01335 + 0.80812 \times 10^{-6}$ 1/[Q]	1.65×10^4	0.9995
304	$Y = 0.01327 + 0.90758 \times 10^{-6}$ 1/[Q]	1.46×10^4	0.9996
314	$Y = 0.01296 + 0.97723 \times 10^{-6}$ 1/[Q]	1.33×10^4	0.9996

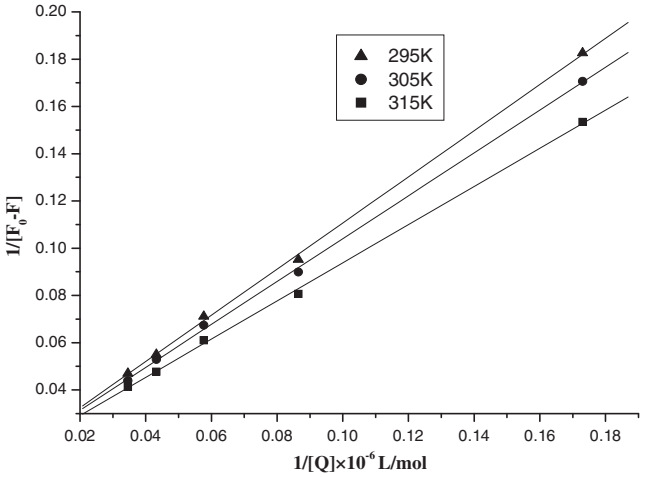

Figure 3. The Lineweaver–Burk curves for quenching of **α1** with HSA.

3.2.2. Binding modes to HSA

Generally, a small molecule binds to a macromolecule by the following four binding modes: hydrogen bonds, van der Waals attractions, electrostatic interactions, and hydrophobic interactions. The thermodynamic parameters, enthalpy change (ΔH) and entropy change (ΔS) of reaction, are very important for confirming binding modes. The temperature-dependence of the binding constant was investigated at three different temperatures (294, 304 and 314 K), considering that HSA could not undergo any structural degradation.

The thermodynamic parameters (Table 3) were determined from the linear Van't Hoff plot (Fig. 6) according to the thermodynamic Eqs. 5 and 6. As shown in Table 3, ΔG and ΔH are negative, and ΔS is positive. So, the formation of the α1–HSA coordination compound is a spontaneous and exothermic reaction accompanied a positive ΔS value. According to the views of Neméthy and Scheraga,[22] Timasheff,[23] and Subramananian,[24] the positive ΔS value is frequently taken as an evidence for hydrophobic interactions. Furthermore, specific electrostatic interactions between ionic species in aqueous solution are characterized by a positive value of ΔS and a negative ΔH value. Accordingly, it is impossible to account for the thermodynamic parameters of the **α1**–HSA compound on the basis of a single molecular interaction. It is more likely that both hydrophobic and electrostatic interactions are involved in the binding process. Thus, electrostatic interactions did not play a major role in the binding, and **α1** bound to HSA mainly based on hydrophobic interactions.

3.2.3. The energy transfer between α1 and HSA

According to Föster's theory,[25,26] the efficiency of energy transfer is related not only to the distance between the tryptophan residue (donor) and the **α1** (acceptor), but also to the critical energy transfer distance. That is,

$$E = 1 - F/F_0 = R_0^6/(R_0^6 + r^6), \tag{8}$$

where r represents the distance between donor and acceptor and R_0 is the critical distance when transfer efficiency is 50%, which can be calculated by

$$R_0^6 = 8.8 \times 10^{-25} k^2 n^{-4} \Phi J, \tag{9}$$

where k^2 is the orientation factor related to the geometry of the donor–acceptor of the dipole, n is the refractive index of medium, Φ is the fluorescence quantum yield of the donor, and J is the spectral overlap of the donor emission and the acceptor absorption. The value J is given by

$$J = \sum F(\lambda)\varepsilon(\lambda)\lambda^4 \Delta\lambda / \sum F(\lambda)\Delta\lambda, \tag{10}$$

where $F(\lambda)$ is the fluorescence intensity of the fluorescence reagent when wavelength is λ, and $\varepsilon(\lambda)$ is the molar absorbance coefficient of the acceptor at the wavelength of λ. From these equations, J, E, and R_0 can be calculated, so the value of r also can be evaluated.

The overlaps of the fluorescence spectrum of HSA and the absorption spectrum of **α1** are shown in Figure 4. The overlap integral calculated according to the above relationship is 1.734×10^{-14} cm^3 L mol^{-1} for HSA. It has been reported that $k^2 = 2/3$, $n = 1.336$, $\Phi = 0.118$ for HSA. Based on these data, the distance between **α1** and the tryptophan residue in HSA is 4.06 nm. Obviously, it is lower than 7 nm after interaction, which is in accordance with conditions of Föster's non-radiative energy-transfer theory. It indicated that the energy transfer happened when binding between **α1** and HSA, and energy transfer may depend on the distance between the tryptophan residue and **α1** bound to HSA.

3.2.4. Identification of binding sites on HSA and molecule modeling

Descriptions of the 3D structure of crystalline albumin show that HSA comprises three homologous domains (I–III): I (residues 1–195), II (196–383), III (384–585), each of which can be divided into two subdomains (A and B). HSA has a limited number of binding sites for endogenous and exogenous ligands that are typically bound reversibly and have binding constants in the range of 10^4–10^8 M^{-1}.[27] Sudlow et al.[28] have suggested that there are two main distinct binding sites on HSA, site I and site II, which locate in the hydrophobic cavities of sub-domains IIA and IIIA, respectively, and one tryptophan residue (Trp-214) of HSA is in subdomain IIA.[29] There is a large hydrophobic cavity present in subdomain IIA to which many drugs can bind.

The best energy-ranked result is shown in Figure 5. The **α1** molecule was located within the binding pocket and was adjacent to

Table 3
The thermodynamic parameters for the binding **α1** to HSA

T (°C)	ΔG (kJ mol^{-1})	ΔH (kJ mol^{-1})	ΔS (J mol^{-1} K^{-1})
294	−23.74		
304	−24.24	−8.26	52.60
314	−24.79		

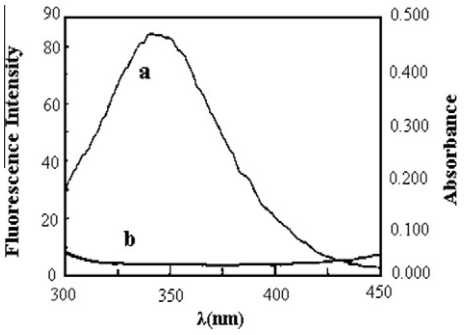

Figure 4. The overlap of UV absorption spectrum of **α1** with the fluorescence emission spectrum of HSA. (a) The fluorescence emission spectrum of HSA (8×10^{-7} M); (b) The UV absorption spectrum of **α1** (5.78×10^{-6} M).

hydrophobic residues such as TRP-214, PHE-223, LEU-238, LEU-260, ILE-264, and ILE-290 of HSA. The result suggested the existence of hydrophobic interactions between them. Furthermore there were also a number of specific electrostatic interactions and hydrogen bonds, because several ionic and polar residues in the proximity of the ligand play an important role in stabilizing the α**1** molecule via H-bonds and electrostatic interactions. There were hydrogen interactions between H (NH_2) of the α**1** molecule and the residues LYS-195, 5′-O and ARG-218, 5-O and ARG-222, 6-O and ARG-222, 11-O and HIS-242, 12-O and HIS-242, H (3″-OH) and GLU-292 of HSA. The results suggested that the formation of hydrogen bonds decreased the hydrophilicity and increased the hydrophobicity to keep stability in the α**1**–HSA system. Therefore, the results of modeling indicated that the interaction between α**1** and HSA was dominated by hydrophobic forces, which was in accord with the binding mode study.

3.2.5. Conformation investigation

Synchronous fluorescence spectra give information about the molecular environment in a vicinity of the chromosphere molecules and have several advantages, such as sensitivity, spectral simplification, spectral bandwidth reduction, and the avoidance of different perturbing effects.[29] Yuan et al.[30] have provided a useful method to study the environment of amino acid residues by measuring the possible shift in wavelength emission maximum k_{max}, the shift in position of emission maximum corresponding to the changes of the polarity around the chromophore molecule. When the *D*-value ($\Delta\lambda$) between the excitation wavelength and emission wavelength were stabilized at 15 or 60 nm, the synchronous fluorescence gave the characteristic information of tyrosine residues or tryptophan residues.[31] To explore the structural change of HSA by the addition of α**1**, the synchronous fluorescence spectra (Fig. 6) of HSA with various amounts of α**1** were measured. The effect of α**1** on HSA synchronous fluorescence spectroscopy is shown in Figure 6. It is apparent that there is a small red shift of tryptophan residues fluorescence upon addition of the drug, whereas the emission maximum of tyrosine kept its position. The red shift of the emission maximum indicates that the conformation of HSA has changed, the polarity around the tryptophan residues has increased and the hydrophobicity is decreased.[32]

UV–vis absorption measurement is a very simple method and one that is applicable for exploring the structural changes[29] and to signal the complex formation.[33] For reconfirming the structural change of HSA by addition of α**1**, the UV–vis absorbance spectra of HSA with various amounts of α**1** was also measured and is displayed in Figure 7. The baselines of the UV–vis absorbance spectra at 320–200 nm were raised and the absorption spectral maximum showed a blue shift (from 256 to 249 nm), indicating that an interaction had occurred between α**1** and HSA. Thus the HSA molecules associated with α1 to form an α**1**–HSA complex, while the peptide strands of HSA molecules extended even more and the hydrophobicity was decreased. This conclusion agrees with the results of the conformational changes by synchronous fluorescence spectra, which indicate that the approach using synchronous fluorescence spectroscopy is scientifically valid.[29]

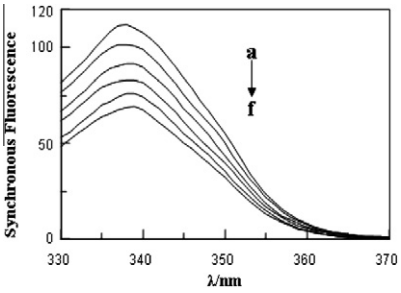

Figure 6. Synchronous fluorescence spectrum of HSA with α**1** (T = 295 K, pH 7.40), $c_{HSA} = 1.2 \times 10^{-6}$ M, c(α**1**)/(10^{-6} M), a–f: 0, 5.78, 11.56, 17.34, 23.12, 28.90.

3.2.6. Effect of co-ions on binding of α1 to HSA

Previous studies indicated that HSA has a high affinity metal-binding site at the N-terminus. The multiple binding sites underlie the exceptional ability of HSA to interact with many organic and inorganic molecules and make this protein an important regulator of intercullar fluxes and the pharmacokinetic behavior of many drugs.[34] Therefore, it is of interest to examine the effect of inorganic cations and anions in the solution system of α**1**–HSA. The effect of common ions on the binding constants at 295 K is listed in Table 4. As shown in Table 4, the binding constants between α**1** and protein have changed in the presence of common ions, implying some binding between metal ions and HSA. This confirmed that the presence of metal ions directly affected the binding between α**1** and HSA. As a result, the competition between coexistent ions and α**1** decreases the binding constant between α**1** and HSA, which causes a shortening of the lifetime of α**1** in blood plasma and enhances the maximum effectiveness of the drug.

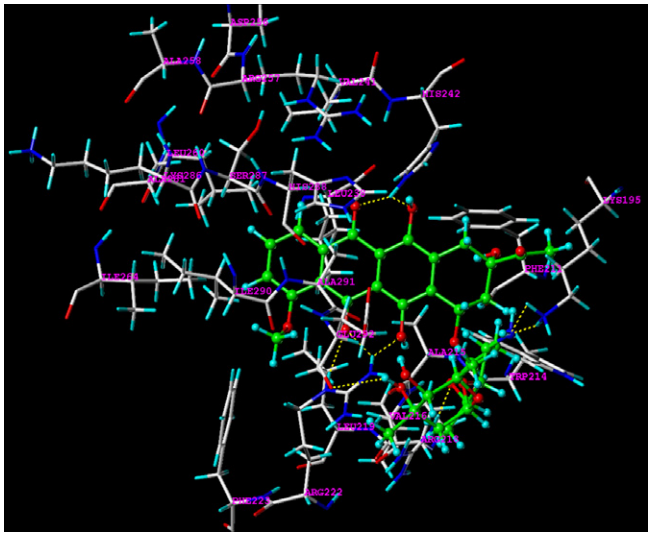

Figure 5. The interaction model between α**1** and HSA, The residues of α**1** and HSA are represented using different colored stick models. The hydrogen bond between the ligand and the protein is indicated by a dashed line.

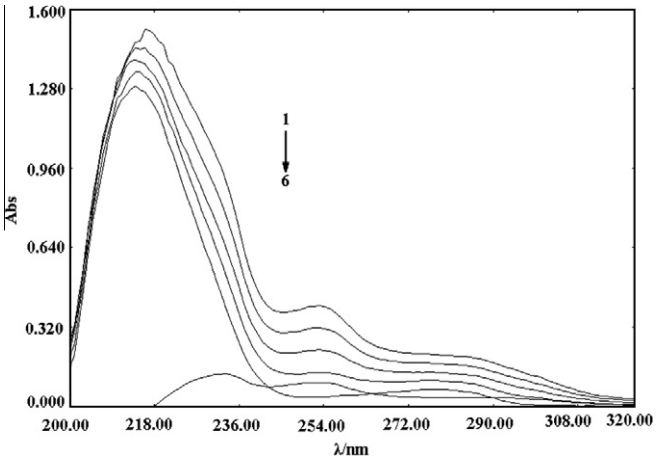

Figure 7. UV absorption spectra of HSA in the absence and presence of α**1**.

Table 4
The binding constants between α**1** and HSA in the presence of other ions

Ions	K ($\times 10^4$)	R	Ions	K ($\times 10^4$)	R
Zn^{+}	0.62	0.9994	Cd^{2+}	0.14	0.9989
SO_4^{2-}	1.43	0.9992	Hg^{2+}	0.63	0.9992
CO_3^{2-}	0.31	0.9995	Al^{3+}	0.15	0.9986
PO_4^{3-}	1.16	0.9988	Cl^{-}	0.10	0.9990
Mg^{2+}	1.19	0.9998	Mn^{2+}	0.42	0.9992
F^{-}	1.14	0.9999	Pb^{2+}	1.01	0.9988

4. Conclusions

An improved approach to the title compound α**1** has been developed that gives high selectivity and good yield. Studies on the interaction of α**1** with HSA show that the intrinsic fluorescence of HSA is quenched through a static quenching mechanism, and the binding of α**1** to HSA is predominantly due to hydrophobic interactions estimated from the signs of ΔH and ΔS. These findings are consistent with the results from a molecular modeling study. The binding of α**1** to HSA can induce a conformational change of HSA, which is proved by the qualitative analysis data of synchronous fluorescence spectra. This study also indicates that α**1** is a strong quencher and is bound to HSA with high affinity. These results and theoretical data indicate that α**1** could bind to HSA and be effectively transported and eliminated in the body. Such findings may provide be a useful guidelines for further drug design.

Acknowledgments

This work was supported by the National Natural Science Foundation of China (20872029, 30970696), the program for Innovative Research Team (in Science and Technology) in University of Henan Province (2008IRTSTHN002), and Innovation Scientists and Technicians Troop Construction Projects of Henan Province (084100510002) to G.Z.

References

1. Arcamone, F. *Doxorubicin, Anticancer Antibiotics* In *Medicinal Chemistry Series*; Academic Press: New York, 1981; Vol. 17, pp 1–369.
2. Zhang, G.; Fang, L.; Zhu, L.; Aimiuwu, J. E.; Shen, J.; Chen, H.; Muller, M. T.; Lee, G. E.; Sun, D.; Wang, P. G. *J. Med. Chem.* **2005**, *48*, 5269–5278.
3. Battisti, R. F.; Zhong, Y.; Fang, L.; Gibbs, S.; Shen, J.; Nadas, J.; Zhang, G.; Sun, D. *Mol. Pharmacol.* **2007**, *4*, 140–153.
4. He, X. M.; Carter, D. C. *Nature* **1992**, *258*, 209–215.
5. Olson, R. E.; Christ, D. D. *Annu. Rep. Med. Chem.* **1996**, *31*, 327–336.
6. Tang, J. H.; Qi, S. D.; Chen, X. G. *J. Mol. Struct.* **2005**, *779*, 87–95.
7. Carter, D. C.; Ho, J. X. *Adv. Protein Chem.* **1994**, *45*, 153–203.
8. Mathias, U.; Jung, M. *Anal. Bioanal. Chem.* **2007**, *388*, 1147–1156.
9. Otagiri, M.; Masuda, K.; Imai, T.; Imamura, Y.; Yamasaki, M. *Biochem. Pharmacol.* **1989**, *38*, 1–7.
10. Sułkowska, A. *J. Mol. Struct.* **2002**, *614*, 227–232.
11. Ware, W. R. *J. Phys. Chem.* **1962**, *66*, 455–458.
12. Hu, Y. J.; Liu, Y.; Zhang, L. X. *J. Mol. Struct.* **2005**, *750*, 174–178.
13. Sharma, A.; Schulman, S. G. *Introduction of Fluorescence Spectroscopy*; John Wiley & Sons: New York, 1999; pp 237–248.
14. Tian, J. N.; Liu, J. Q.; He, W. Y.; Hu, D.; Chen, X. G. *Biomacromolecules* **2004**, *5*, 1956–1961.
15. Rubio, S.; Gomez-Hens, A.; Ualcarcel, M. *Talanta* **1986**, *33*, 633–640.
16. Cui, F. L.; Fan, J.; Li, J. P.; Hu, Z. D. *Bioorg. Med. Chem.* **2004**, *12*, 151–157.
17. Hua, Y. J.; Liu, Y.; Wang, J. B.; Xiao, X. H.; Qu, S. S. *J. Pharm. Biomed. Anal.* **2004**, *36*, 915–919.
18. Cui, F.; Yan, Y.; Zhang, Q.; Du, J.; Yao, X.; Qu, G.; Lu, Y. *Carbohydr. Res.* **2004**, *314*, 189–199.
19. SYBYL *Software, Version 6.9*; Tripos Associates: St. Louis, 2003.
20. Silva, D.; Cortez, C. M.; Bastos, J. C. *Toxicol. Lett.* **2004**, *147*, 53–61.
21. Petitpas, I.; Grune, T.; Bhattacharya, A. A. *J. Mol. Biol.* **2001**, *314*, 955–960.
22. Neméthy, G.; Scheraga, H. A. *J. Phys. Chem.* **1962**, *66*, 1773–1789.
23. Timasheff, S. N. Thermodynamic of Protein Interactions. In *Proteins of Biological Fluids*; Peeters, H., Ed.; Pergamon Press: Oxford, 1972; pp 511–519.
24. Ross, P. D.; Subramanian, S. *Biochemistry* **1981**, *20*, 3096–3102.
25. Förster, T. In *Modern Quantum Chemistry*; Sinanoglu, O., Ed.; Academic Press: New York, 1996; Vol. 3,.
26. Lakowicz, J. R. *Principles of Fluorescence Spectroscopy*; Plenum Press: New York, 1983. Chapter 10.
27. Peters, T. *All About Albumin* In *Biochemistry, Genetics and Medical Application*; Academic Press: San Diego, 1996.
28. Sudlow, G.; Birkett, D. J.; Wade, D. N. *Mol. Pahrmacol.* **1976**, *12*, 1052–1061.
29. Hu, Y. J.; Liu, Y.; Pi, Z. B.; Qu, S. S. *Bioorg. Med. Chem.* **2005**, *13*, 6609–6614.
30. Yuan, T.; Weljie, A. M.; Vogel, H. J. *Biochemistry* **1998**, *37*, 3187–3195.
31. Abert, W. C.; Gregory, W. M.; Allan, G. S. *Anal. Biochem.* **1993**, *213*, 407–413.
32. Klajnert, B.; Bryszewska, M. *Bioelectrochemistry* **2002**, *55*, 33–35.
33. Bi, S. Y.; Song, D. Q.; Tian, Y.; Zhou, X.; Liu, X.; Zhang, H. Q. *Spectrochim. Acta, Part A* **2005**, *61*, 629–636.
34. Maruyama, A.; Lin, C. C.; Yamasaki, K.; Miyoshi, T.; Imal, T.; Yamasaki, M.; Otagiri, M. *Biochem. Pharmacol.* **1993**, *45*, 1017–1026.